EXPERIMENTAL IMPLEMENTATION OF SS 316L CRUCIFORM TESTING TO ACHIEVE VARIOUS DEFORMATION PATHS

Elizabeth M. Mamros*, Sarah M. Mayer, Jinjin Ha, and Brad L. Kinsey

University of New Hampshire, Durham, NH, 03824, USA *Corresponding Author, emm1109@wildcats.unh.edu

Keywords: Forming, Deformation path, Biaxial loading, Stainless steel, Cruciform

Abstract

By following varying deformation paths, e.g., a linear path to equibiaxial loading versus a bilinear path of uniaxial loading followed by biaxial loading, the same final strain state can be achieved. However, the stress state that the material is subjected to is considerably different due to the varying deformation. This is of interest in a growing field of stress superposition to improve formability and manipulate final part properties in metal forming applications. One potential application is forming patient-specific, trauma fixation hardware with differing strength and weight reduction requirements in various regions. In this paper, experiments were performed on a custom fabricated cruciform machine with the goal of subjecting stainless steel 316L to various deformation paths. A novel cruciform specimen geometry was designed in collaboration with the US National Institute of Standards and Technology to achieve large strain values in the gauge region. Digital Image Correlation was utilized to measure surface strain fields in real time.

1. Introduction

Due to both work hardening and possible phase transformations during forming, the initial material properties are not necessarily representative of the properties in the processed part. Conventional experiments for the material characterization, including uniaxial tension, and basic constitutive laws do not capture the material behavior correctly under complex and varying loading paths that are often intrinsic to forming processes [1].

In order to capture such complex loading experimentally, Shiratori and Ikegami proposed the cruciform biaxial tension experimental procedure in 1967 [2]. In contrast to hemispherical dome tests (another technique for biaxial loading experimentation), cruciform tests do not involve a pressurization effect, allow the same specimen geometry to be used for all experiments, and enable the deformation path to be varied during a test [3]. In recent decades, several biaxial cruciform machines have been developed, some of which are summarized in [3], but, thus far, an ASTM standard for the cruciform specimen geometry does not exist. Common problems that arise when designing cruciform specimens include early failure in the arms, low strain values at failure, and a non-homogeneous strain distribution in the gauge area.

Austenitic stainless steels (SS) undergo stress-induced phase transformation to martensite during forming, particularly at low temperatures and high strains [4]. Hecker et al. found that for the case of balanced biaxial tension of SS 304L, the degree of martensitic transformation is more than twice the amount observed, per maximum

principal strain value, during uniaxial tension [5]. Thus, characterization of the transformation kinetics at various proportional loading paths is required to determine the deformation path most beneficial in terms of stress superposition.

In this paper, SS 316L specimens were loaded on a custom cruciform frame [7] designed to implement non-linear deformation paths. A custom cruciform specimen able to achieve large strain values in the gauge area was created in collaboration with the US National Institute of Standards and Technology (NIST) via a previously used methodology [1, 6]. The three loading paths investigated, 4:4 (equibiaxial), 4:2, and 4:0, were applied as constant displacement ratios between the perpendicular axes ($\Delta Y: \Delta X$). The area of interest on the specimen, i.e., the flat surface within the pocket in the gauge area, was chosen to capture a region containing relatively uniform deformation. Digital Image Correlation (DIC) was used to measure the strains *in-situ*. The martensitic transformations of SS 316L will be measured using electron backscatter diffraction (EBSD) with the scanning electron microscope, but this is outside of the scope of this paper.

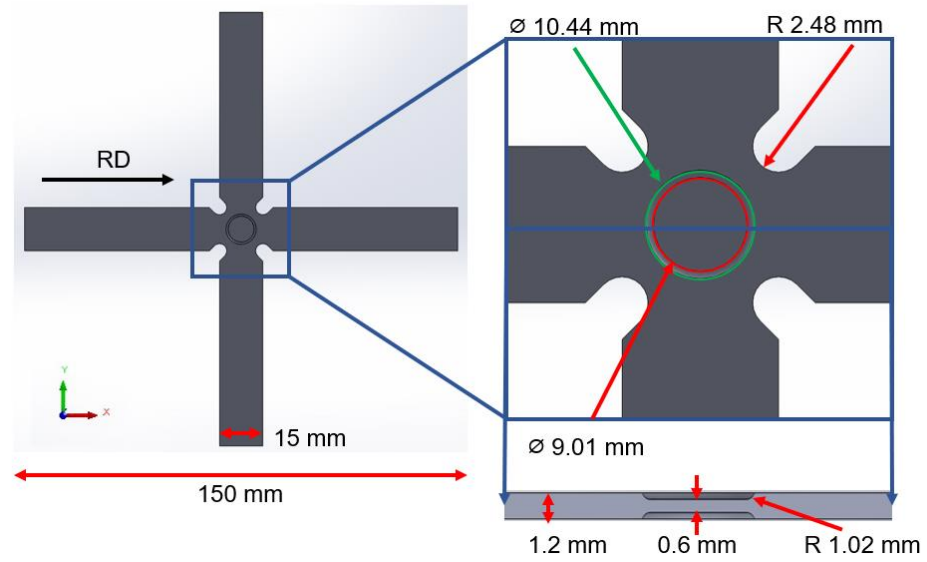


Figure 1. Overall cruciform specimen geometry obtained from 1.2 mm thick SS 316L [8].

2. Experimental Setup and Methods

2.1 Material and Specimen Preparation

SS 316L, a biocompatible material, with a thickness of 1.2 mm was used in this study. In collaboration with NIST, a cruciform specimen geometry was designed based on past research [1, 6]. The slightly modified design objectives were to create a specimen that could be manufactured in-house, i.e., with waterjet cutting and milling operations, and achieve both a high equivalent plastic strain and a homogeneous strain distribution in the gauge area. The high equivalent plastic strain threshold was targeted to enhance the amount of martensitic phase transformations, a microstructural change that is common in austenitic stainless steels, including 316L, with large deformations. The homogeneous strain distribution in the gauge area will be critical for accurate martensitic transformation measurements. The specimens were oriented with arms parallel to the rolling and transverse directions, and the profile was waterjet cut (see Figure 1). The edges were

sanded prior to testing. A 4 mm diameter end mill was used on each side of the specimen to machine the pocket in the gauge section. The fabricated specimen dimensions were measured using a confocal microscope (Olympus OLS5000-SAF) to confirm that all desired tolerances were achieved.

NIST has investigated this specimen geometry during previous research [1, 6], but in order to use this geometry in conjunction with the cruciform machine at UNH, modifications were required. Two key factors necessitating this geometry study were accounting for the size difference between the testing equipment and meeting the desired minimum equivalent plastic strain threshold of 30% in the center pocket. Table 1 lists the dimensions used to fabricate the specimens at UNH. Figure 2 shows a schematic of the cruciform specimen geometry with dimensions that correspond to the values in Table 1.

Dimension	Value (mm)
Gauge Thickness, T _{pocket}	0.60
Sheet Thickness, T _{sample}	1.20
Fillet, F _{pocket}	1.02
Flat Area Radius, R _{gauge}	4.51
Pocket Diameter, Dpocket	10.44
Arm Width, W _{arm}	15.00
Notch Radius, R _{notch}	2.48
Notch Diameter, Dnotch	4.96
Diagonal	21.21

Table 1. Cruciform geometry dimensions.

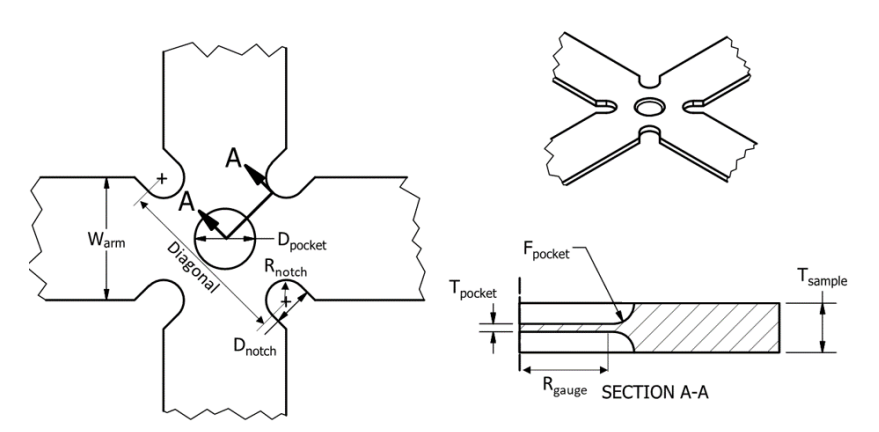


Figure 2. Schematic of final cruciform specimen geometry (modified from [6]).

2.2 Cruciform Machine

A cruciform machine capable of applying biaxial tension along perpendicular axes was constructed at UNH in collaboration with Prof. Kuwabara at the Tokyo University of Agriculture and Technology [9] (see Figure 3). The loading is applied via four Parker 3LX Series hydraulic cylinders (see Table 2 for key specifications). Greenerd Press and Machine Co. designed and built the hydraulic system and control circuitry. The machine can displace the opposing cylinders equally within 0.1 mm of the programmed value at a

maximum velocity of 80 mm/min. A human-machine interface was programmed in LabVIEW software to control the machine.

Parameter	Value
Maximum Pressure	9.65 MPa
Bore Diameter	63.5 mm
Stroke	12.7 mm
Maximum Tensile Force	25.8 kN
Maximum Compressive Force	30.7 kN

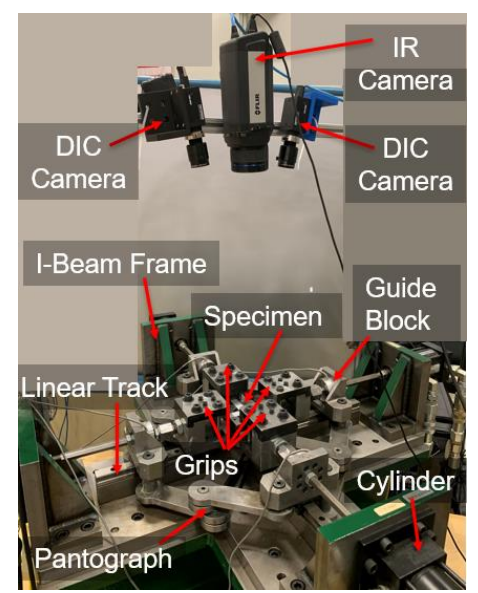


Figure 3. UNH cruciform machine.

2.3 Digital Image Correlation

To capture strain measurements in-situ, two FLIR 8.9 megapixel cameras with 50 mm Schneider Xenoplan compact lens were used (see Figure 3) for 3D DIC analyses. The specimens were prepared with a white background and overlaid black speckle pattern using spray-paint. The images were post processed in VIC-3D from Correlated Solutions, Inc. with subset, step, and filter sizes of 21, 5, and 5 pixels respectively. The area of interest selected was the ~9 mm diameter flat region in the gauge section. The temperature increase during these experiments, captured by the FLIR SC-645 infrared camera, was <15°C, and thus, further temperature data is not presented in this work.

2.4 Biaxial Experiments

The biaxial experiments were conducted on the cruciform machine by programming displacements and pulling speeds in each axis. A removable fixture to ensure consistent specimen placement and proper alignment in the grips was designed and 3D-printed (see Figure 4). For consistency, the arms oriented along the rolling direction (RD) were positioned parallel to the x-axis for each experiment. For equibiaxial conditions, a total displacement of 10 mm, i.e., 5 mm along each arm, and pulling speed of 0.1 mm/s were

prescribed to each axis. For the other loading conditions, the pulling speed of the x-axis was decreased according to the desired displacement to ensure that the displacement ramps would terminate at the same time. The strain rate along each axis for all experiments was approximately $10^{-3} - 10^{-4} \, \text{s}^{-1}$. Three experiments were completed for each displacement case of interest to verify repeatability.

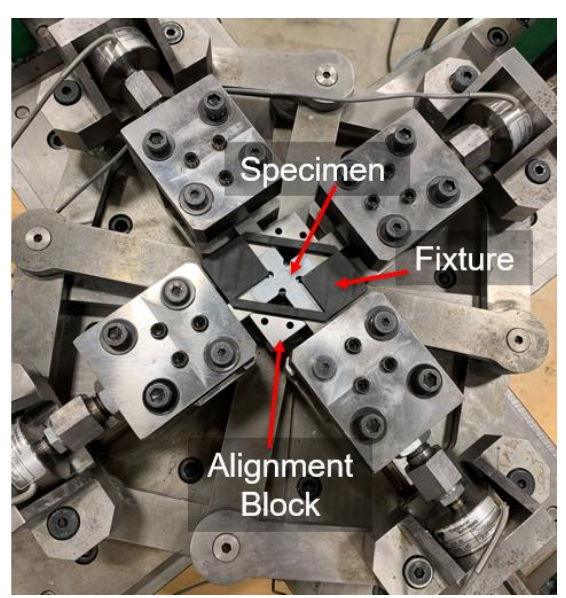


Figure 4. Specimen alignment fixture on cruciform machine.

3. Results and Discussion

3.1 Force vs Displacement Results

During each experiment, the biaxial cruciform machine recorded force and displacement data for each axis from the load cells and embedded linear variable displacement transducers, respectively. The displacement values presented represent the displacement along the positive axes, i.e., the total displacement for each axis is twice the stated value. Figure 5 summarizes these results for all displacement paths. Comparing the maximum displacements along the y-axis (TD), the 4:0 path had the largest value, followed by the 4:2 path, and the 4:4 path had the smallest value as expected. With respect to the y-axis (TD), the maximum force values follow the same trend for the three displacement paths presented.

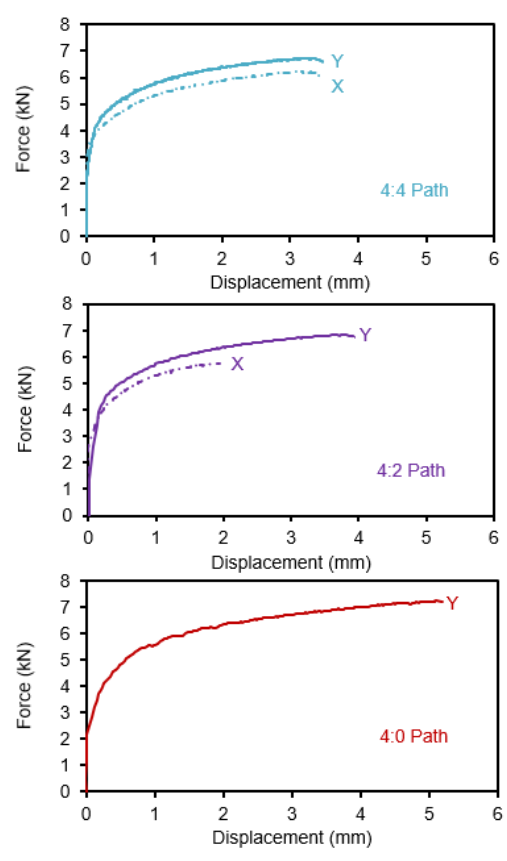


Figure 5: Force-displacement curves for all 4:4, 4:2, and 4:0 displacement paths.

3.2 Strain Results

Table 3 shows the true strain values onset of fracture at the center point of the specimen geometry. The corresponding strain paths, ε_{yy} versus ε_{xx} , are shown in Figure 6. The strain contours and values at the center point for the x-direction and y-direction are nearly equivalent as expected for the equibiaxial case, with variations being due to the anisotropy of the material. The 4:2 path had a slightly larger true strain along the y-direction than the 4:0 path, but the 4:0 path exhibited a much larger equivalent von Mises strain than the 4:2 path.

Table 3. DIC true strain results from the image prior to fracture for 4:4, 4:2, and 4:0 displacement paths.

	Value at Center Point (mm/mm)		
True Strain	4:4 Path	4:2 Path	4:0 Path
ε_{xx}	0.188	0.127	-0.136
$arepsilon_{yy}$	0.185	0.249	0.233
ε_{VM}	0.189	0.218	0.323

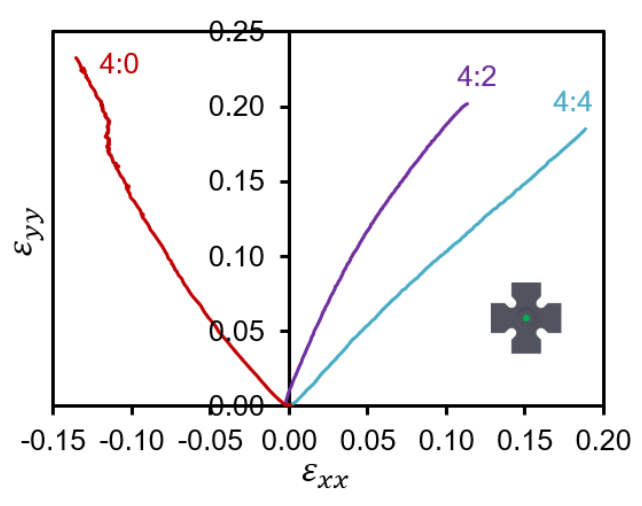


Figure 6. True strain paths extracted from DIC analyses at the center of the specimen for 4:0, 4:2, and 4:0 displacement paths.

The strain distributions in the gauge area are shown in Figure 7. The strain contours show that the equivalent von Mises strain is >30% within the gauge region, not necessarily at the center point, for all displacement paths. This indicates that significant martensitic transformation is expected in the corresponding locations.

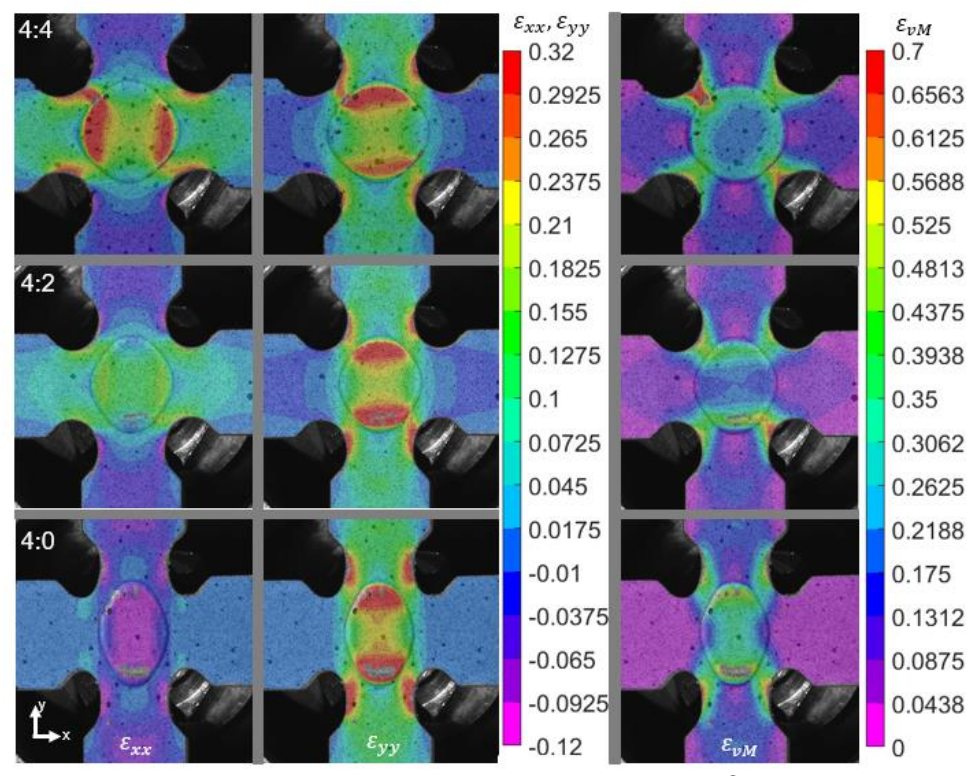


Figure 7. True strain distribution immediately prior to fracture: x-direction, y-direction, and von Mises for 4:4, 4:2, and 4:0 displacement paths.

4. Conclusion and Future Work

Initial experimental results from SS 316L cruciform specimens deformed with 4:4, 4:2, and 4:0 displacement paths have been presented. The resulting strain values were determined with 3D DIC and indicate the propensity for martensitic transformation. Future experiments will be conducted to investigate varying deformation paths and to determine the relationship between a specific non-linear deformation path and the induced martensitic transformations measured by EBSD. An analytical model will also be developed to determine multiple non-linear deformation paths that will result in the same final strain state but hypothesized differing martensite volume fractions.

5. Acknowledgements

The authors would like to thank Mark Iadicola and Dilip Banerjee from NIST for their assistance in designing this cruciform specimen. The Olympus confocal microscope used is managed by the University Instrumentation Center (UIC) at the University of New Hampshire (UNH). Support for the NH BioMade Project is provided by the US National Science Foundation EPSCoR award (#1757371).

5. References

- [1] Creuziger A, ladicola MA, Foecke T, Rust E, and Banerjee D. Insights into Cruciform Sample Design. JOM (1989). 2017; 69(5):902–906. doi:10.1007/s11837-017-2261-6
- [2] Shiratori E and Ikegami K. A new biaxial tensile testing machine with flat specimen. Bulletin of the Tokyo Institute of Technology (1967) 82:105–118.
- [3] Xiao, R. A review of cruciform biaxial tensile testing of sheet metals. Experimental Techniques (2019) 43: 501. doi.org/10.1007/s40799-018-00297-6
- [4] Lichtenfeld, JA, Van Tyne, CJ, and Mataya, MC. Effect of strain rate on stress-strain behavior of alloy 309 and 304L austenitic stainless steel. Metallurgical and Materials Transactions A (2006) 37: 147. doi.org/10.1007/s11661-006-0160-5
- [5] Hecker, SS, Stout, MG, Staudhammer, KP, and Smith, JL. Effects of Strain State and Strain Rate on Deformation-Induced Transformation in 304 Stainless Steel: Part I. Magnetic Measurements and Mechanical Behavior. Metallurgical Transactions A (1982) 13A: 619-26.

- [6] Iadicola, MA, Creuziger, AA, and Foecke, T. Advanced biaxial cruciform testing at the NIST Center for Automotive lightweighting. Rossi, M, Sasso, M, N. Connesson, Singh, R, DeWald, A, Backman, D, et al. (Eds.), Residual Stress, Thermomechanics & Infrared Imaging, Hybrid Techniques and Inverse Problems, 8, Springer International Publishing (2014), pp. 277-285.
- [7] Wilson, JF. Development of a biaxial loading frame for thin sheet cruciform specimens. Master's Theses and Capstones, University of New Hampshire (2015) 1027. scholars.unh.edu/thesis/1027
- [8] Mamros, EM, Eaton, MC, Ha, J, and Kinsey, BL. Numerical analysis of SS316L biaxial cruciform specimens under proportional loading paths. Proceedings of ASME Manufacturing Science and Engineering Conference (2021).
- [9] Deng, N, Kuwabara, T, and Korkolis, YP. Cruciform specimen design and verification for constitutive identification of anisotropic sheets. Experimental Mechanics (2015) 55: 1005. doi.org/10.1007/s11340-015-9999-y